Table 1. Basic Characteristics of Study Subjects

	Case	Control
GWAS		
Platform	Illumina HumanHap550	Illumina HumanHap550
Number of samples	372	3389
Ethnicity	Japanese	Japanese
Male (%)	266 (71.5)	1846 (54.5)
Age at sampling, y[a]	33.8 ± 9.3	52.5 ± 15.2
Replication		
Platform	Multiplex PCR ad Invader assay	Illumina HumanHap550 Illumina Human Hap610-Quad
Number of samples	1151	15,800
Ethnicity	Japanese	Japanese
Male (%)	789 (68.6)	10,427 (66.0)
Age at sampling, y[a]	34.4 ± 13.9	63.7 ± 10.5

[a]Mean ± standard deviation.

creases the risk for ulcerative colitis (MIM 191390) but confers a protective effect for CD.[21] Here, we report a GWAS using 372 individuals with CD and 3389 controls with a replication analysis of the top associations in an independent panel of 1151 Crohn's disease cases and 15,800 controls.

Patients and Methods

Subjects Enrolled in the Study

A total of 1535 individuals with CD and 19,283 control subjects were enrolled in this study. All individuals were of Japanese descent. Characteristics of the study subjects are shown in Table 1. CD cases for the GWAS were collected at the Social Insurance Chuo General Hospital (n = 376; same set as the previous study[21]). Cases for the replication study were a total of 1159 subjects collected at the Social Insurance Chuo General Hospital (n = 160), Toho University Sakura Medical Centre (n = 41), Sapporo Medical University School of Medicine and Sapporo Kosei Hospital (n = 351), and Kyushu University and 16 affiliated hospitals (n = 607). All CD cases were diagnosed by expert gastroenterologists in accordance with clinical, radiologic, endoscopic, and histologic features according to the Lennard-Jones[22] criteria. Patients with indeterminate colitis were excluded. The control subjects for the GWAS consisted of 3397 subjects from 2 groups, healthy volunteers (n = 906) recruited at the Midosuji and other related Rotary Clubs,[6,20,21,23] and subjects (n = 2491) obtained from the BioBank Japan project (http://biobankjp.org/) who had been enrolled based on having one of various disease classes (cervical cancer, esophageal cancer, gallbladder cancer, liver cancer, ovarian cancer, pancreatic cancer, hematologic cancer, endometrial cancer, chronic hepatitis B, keloid, drug eruption, febrile seizure, and pulmonary tuberculosis).[24] For replication study controls, we used a nonoverlapping set of samples from the BioBank Japan project that consisted of 15,800 individuals classified into 1 of 10 disease categories (colorectal cancer, breast cancer, prostate cancer, lung cancer, stomach cancer, diabetes, arteriosclerosis obliterans, atrial fibrillation, cerebral infarction, and myocardial infarction). The study was approved by the ethical committees of each participating medical center, the Institute of Medical Science, the University of Tokyo, and the Riken Yokohama Institute.

Single-Nucleotide Polymorphism Genotyping and Quality Controls

In the GWAS, 376 CD cases and 3397 controls were genotyped using the Illumina HumanHap550v3 Genotyping BeadChip (Illumina). We excluded 2 CD cases with call rates lower than 0.98. After searching for close relatives using identity-by-descent estimated by PLINK (available at http://pngu.mgh.harvard.edu/~purcell/plink/), we excluded 2 cases and 8 control subjects. To evaluate potential stratification in our study population, we merged the GWAS data with European (CEU; Utah residents [CEPH] with Northern and Western European ancestry), African (YRI; Yoruba in Ibadan, Nigeria), and East-Asian (Japanese and Han Chinese; JPT; Japanese in Tokyo, Japan and CHB; Han Chinese in Beijing, China) individuals' genotype data obtained from the Phase II HapMap database (release 22)[25] and performed a principal component analysis (PCA). A PCA plot clearly separated the subjects into 3 clusters as previously described (Supplementary Figure 1).[26] We applied stringent quality control criteria to the single-nucleotide polymorphism (SNP) data, with a genotype call rate of 0.99 or greater in both cases and controls, Hardy–Weinberg equilibrium (HWE) $P \geq 1 \times 10^{-6}$ in controls, and minor allele frequency (MAF) greater than 0.01 in both cases and controls. After quality control filtering, a total of 453,099 SNPs consisting of 442,912 autosomal and 10,187 chromosome X SNPs were used for further analysis.

For the replication study, we selected 98 SNPs with $P < 1 \times 10^{-4}$ in the GWAS after excluding SNPs located in previously reported loci in the Japanese population.[6,27] After calculating r^2 among the 98 SNPs we examined groups of SNPs with $r^2 \geq 0.9$ to other candidate SNPs and selected the 65 SNPs that had the lowest P value within each putative locus. Among them, 1 SNP (rs6739399) was excluded because genotype data for controls were not available in the replication set. Another SNP (rs6966614) was excluded because of the difficulty of assay design. A total of 63 SNPs were genotyped using the multiplex polymerase chain reaction (PCR)-based Invader assay (Third Wave Technologies, Madison, WI). We excluded 8 cases with call rates less than 0.98 in the replication study. The concordance rate between genotypes determined by the Illumina HumanHap550v3 BeadChip and those by the Invader assay among 372 duplicated samples in 30 SNPs was 99.90%. The controls for the replication study were genotyped using the Illumina HumanHap610-Quad BeadChip. Genotype concordance between HumanHap550v3 and HumanHap610-Quad BeadChips was 99.99% among 182 duplicate samples, indicating a low possibility of genotype error. As a result, 63 SNPs were analyzed in 1151 cases and 15,800 controls in the replication study.

Genome-Wide Imputation and Replication Analysis

By using IMPUTE2 (available at http://mathgen.stats.ox.ac.uk/impute/impute_v2.html),[28] genome-wide imputation was conducted separately for the 3738 GWAS subjects (372 cases and 3366 controls). The reference haplotypes consisted of data for 286 East-Asian subjects (CHB, 97; CHS, 100; JPT, 89) from the 1000 Genomes Project March 2012 release (phase 1, version 3).[29] The GWAS samples' imputed genotype data had 4,929,034 SNPs with an MAF of more than 5% and an estimated imputation accuracy of greater than 0.9 (IMPUTE2 info).

From analysis of the imputed GWAS data, we found 44 additional candidate lead SNPs representing putative novel susceptibility loci for CD ($P < 1 \times 10^{-4}$). We performed genotyping

of cases in the GWAS panel and estimated the accuracy between imputed and real genotypes by the square of the Pearson product-moment correlation coefficient (R^2).[30] We excluded a total of 10 SNPs from the replication analysis: 4 SNPs (rs141300960, rs70964082, rs36174706, and rs145599534) were excluded because of the difficulty of assay design, and 6 SNPs (rs79409596, rs239934, rs10252980, rs12688018, rs61054368, rs10871762) were excluded because they did not meet the accuracy threshold ($r^2 > 0.9$). For replication analysis of the remaining 34 candidates, we performed genotyping of 1158 cases in the replication cohort and examined the association with 15,061 replication controls for which we had imputed genotype data. We calculated combined association statistics using a meta-analysis between the imputed GWAS data and mixed replication data (cases using real genotypes with imputed control data).

Imputation for High-Density Mapping

Imputation of the GWAS genotype data was performed using MACH v1.0[31] for 2 candidate loci including SNPs within an upstream or downstream 0.5-Mb margin. As reference haplotypes, we used genotype data for 286 East-Asian samples (CHB, 97; CHS, 100; JPT, 89) from 1094 individuals from the 1000 Genomes project released in June 2011.[29] In the process of imputation, 50 Markov chain iterations were implemented. To perform high-density mapping, we selected imputed SNPs with P values of less than 1×10^{-4} and tag SNPs based on HapMap Japanese data using Haploview software (available at: http://www.broadinstitute.org/scientific-community/science/programs/medical-and-population-genetics/haploview/downloads) ($r^2 > 0.9$; MAF > 0.05).[32] Genotyping of these SNPs was performed by a multiplex PCR-based Invader assay, and the same criteria for the replication study was applied (SNPs with HWE of $P \geq 0.001$ and samples with a call rate ≥ 0.98). The concordance rate between imputed and assayed genotypes was 99.74% for 4p14 and 99.77% for 13q14.

Pathway, Protein–Protein Interaction, and Text Mining Analyses

To define pathways and networks involved in CD pathogenesis, we selected 22 SNPs: 12 SNPs that showed nominal association in our replication cohort ($P < .05$) and 10 SNPs that showed association in our previous study.[33] First, we used the Gene Relationships Across Implicated Loci (GRAIL) method of literature-based pathway analysis to explore the connections between genes near our candidates.[34] GRAIL was applied to the 22 selected SNPs by using PubMed abstracts published before December 2006 (avoiding potential bias from the investigation of candidate genes stimulated by GWAS), the JPT+CHB Human HapMap, and the hg18 assembly of the human genome. Subsequently, we tested the hypothesis that a protein-protein interaction network built from these loci was enriched significantly for physical interactions by using DAPPLE.[35] We considered 2 categories of direct or indirect interactions and assessed the significance of the enrichment of physical interactions by permutation.

Statistical Analysis

Association analysis was performed by the Cochran-Armitage trend test. Departure from HWE was evaluated using the chi-square test. We decided to use the significance threshold of $P = 5.0 \times 10^{-8}$ for the GWAS and $P = 7.94 \times 10^{-4}$ (calculated as $\alpha = .05$ for 63 tests after the Bonferroni correction) for the replication study. Combined analysis of the GWAS and the replication study was conducted by using the inverse variance-weighted method.[36] Heterogeneity among the studies was determined by using the Breslow-Day test. To estimate population structure, we performed PCA by using EIGENSTRAT version 3.0.[37] To draw the linkage disequilibrium (LD) map, we used Haploview software,[32] and LD was defined according to the published criteria.[38] For the association analysis for imputed genotypes, we used the R Bioconductor package, snpStats (available: http://www.bioconductor.org/packages/2.8/bioc/html/snpStats.html). We estimated the accuracy at each SNP with the square of the Pearson correlation coefficient between imputed and real genotypes (r^2). For general statistical analysis, we used R statistical environment version 2.12.1 (available: http://www.r-project.org/) or PLINK version 1.07.[39] Haplotype frequencies were estimated by using the expectation maximization (E-M) algorithm as implemented in the SNPHAP program (available: http://www.rfcgr.mrc.ac.uk/Menu/Help/snphap/). We estimated *cis*-expression quantitative trait loci (eQTL) signals based on the quantified data of immortalized B-lymphocytes from HapMap JPT data.[40] The data for individual genotypes for eQTL analysis was from the 1000 Genome project and was extracted with VCFtools software.[41]

Results

A Genome-Wide Association Study and a Replication Study of CD

We conducted a GWAS with 376 CD patients and 3397 control subjects in a Japanese population. All subjects were genotyped using the Illumina HumanHap550v3 BeadChip. After applying stringent quality control criteria (see Patients and Methods section), we performed an association analysis of 453,099 SNPs with MAF of 0.01 or greater in both the case and control groups. PCA showed no genetic heterogeneity among cases and controls (Supplementary Figure 1). A quantile-quantile plot (Supplementary Figure 2; including 2 reported loci: the major histocompatibility complex [MHC] region and *TNFSF15*[6,21]) shows the distribution of observed vs expected P values, whereas the corresponding genomic inflation factor (λ_{GC}) of 1.037 suggests a low possibility of false-positive associations resulting from population stratification or cryptic relatedness. Our discovery panel is small compared with the current standards of GWAS; however, the combined study was estimated to have sufficient statistical power (~98.0% for the risk variant; odds ratio [OR], ~1.5; $\alpha = 5.0 \times 10^{-8}$; allele frequency, 0.1).

Our GWAS identified 19 SNPs that showed significant association with CD at the genome-wide level ($P < 5 \times 10^{-8}$). All of these SNPs are located in previously identified regions; 10 SNPs are in the MHC region, and the other 9 SNPs are in the 9q32 region (Figure 1). The top-associated SNP in the MHC region is rs7765379 ($P = 1.17 \times 10^{-15}$; OR, 1.95; 95% confidence interval [CI], 1.65–2.30), which is located between *HLA-DQB1* and *HLA-DQA2*. The most significant SNP in 9q32 is rs6478106 ($P = 1.64 \times 10^{-14}$; OR, 1.82; 95% CI, 1.55–2.12), which is located at the 3′ flanking region of the *TNFSF15* gene.

To identify new susceptibility loci for CD in the Japanese population, we performed a replication study with 1159 independent cases and 15,800 independent controls.

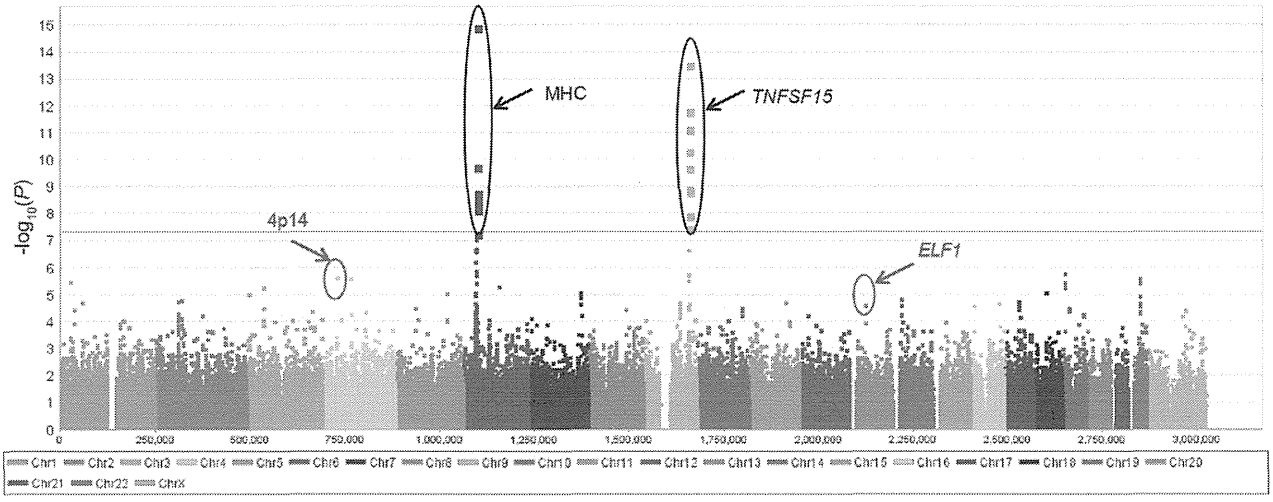

Figure 1. The result of the GWAS for CD. Manhattan plot for 453,099 SNPs from the GWAS for CD. SNPs are plotted according to chromosomal location, with the $-\log_{10}(P)$ calculated by the Cochran–Armitage test. The *red line* indicates the significance threshold for the GWAS ($P = 5.0 \times 10^{-8}$).

Among 98 SNPs with a P value less than 1×10^{-4}, we identified 65 SNPs that represent independent loci after excluding 33 SNPs with strong LD ($r^2 > 0.9$). Among the 65 independent SNPs, 1 SNP (rs6739399) was excluded because genotype data from controls were not available in the replication set. Another SNP (rs6966614) was excluded because of the difficulty of assay design. After applying quality control criteria (see Patients and Methods section), we estimated the association of 63 SNPs successfully genotyped by the multiplex PCR-based Invader assay (Supplementary Table 1). Genotyping success rates in the replication study were 99.93% and 99.99% in cases and controls, respectively. We identified 3 SNPs whose association remained significant after the Bonferroni correction for multiple testing ($P < 7.94 \times 10^{-4}$): rs1487630 on 4p14 ($P = 3.52 \times 10^{-7}$), rs7329174 in the erythroid-like transcription factor family 1 (*ELF1*) on 13q14 ($P = 2.38 \times 10^{-5}$), and rs9891119 in *STAT3* on 17q21 ($P = 2.60 \times 10^{-11}$). The last SNP confirms the association of *STAT3* reported by an early meta-analysis of European subjects.[13] After combining the data from the GWAS and the replication study by using an inverse variance-weighted method, we identified 2 novel susceptibility loci for CD in the Japanese population (rs1487630 on 4p14: $P_{combined} = 1.29 \times 10^{-11}$; OR, 1.33; 95% CI, 1.22–1.44; rs7329174 on 13q14: $P_{combined} = 7.96 \times 10^{-9}$; OR, 1.27; 95% CI, 1.17–1.38) (Table 2). Because rs7329174 is an SNP associated with systemic lupus erythematosus in the Asian population,[42,43] the susceptibility region on 13q14 appears to be a common susceptibility locus for autoimmune diseases in the East-Asian population.

To search for additional candidate loci, we examined associations by using genome-wide imputed genotypes of GWAS samples. This analysis identified 44 candidate variants ($P < 1 \times 10^{-4}$). After applying quality control (see Patients and Methods section), we performed genotyping of 34 SNPs with sufficient accuracy by using 1158 cases in the replication cohort. Association analysis was performed by real genotype data in 1158 cases and imputed genotype data in 15,061 controls. As a result, rs11894081 on 2p25 showed a strong signal for CD in the Japanese population ($P = 3.58 \times 10^{-9}$) (Supplementary Table 2).

Table 2. Summary of Association Analysis With Novel Susceptibility Loci for Japanese CD Patients

SNP region	Gene allele [1/2][a]	Stage	Case			Control			RAF		P^b	OR (95% CI)[c]	$P_{het}{}^d$
			11	12	22	11	12	22	Case	Control			
rs1487630		GWAS	35	156	181	170	1194	2023	0.30	0.23	2.24×10^{-6}	1.49 (1.26–1.76)	
4p14	[T/C]	Replication	93	472	586	941	5652	9206	0.29	0.24	3.52×10^{-7}	1.28 (1.16–1.41)	
		Combined									1.29×10^{-11}	1.33 (1.22–1.44)	.48
rs7329174	*ELF1*	GWAS	32	172	168	213	1241	1935	0.32	0.25	2.32×10^{-5}	1.42 (1.20–1.68)	
13q14	[G/A]	Replication	106	467	578	1071	5908	8821	0.29	0.25	2.38×10^{-5}	1.22 (1.11–1.34)	
		Combined									7.96×10^{-9}	1.27 (1.17–1.38)	.48

RAF; risk allele frequency.
[a]Allele 1 is denoted as the risk allele.
[b]P value was calculated by the Cochrane–Armitage trend test (1 degree of freedom), and combined results were estimated by inverse method-weighted ORs.
[c]Odds ratio of the risk allele is provided as a reference.
[d]Results of Breslow–Day test for the combined data.

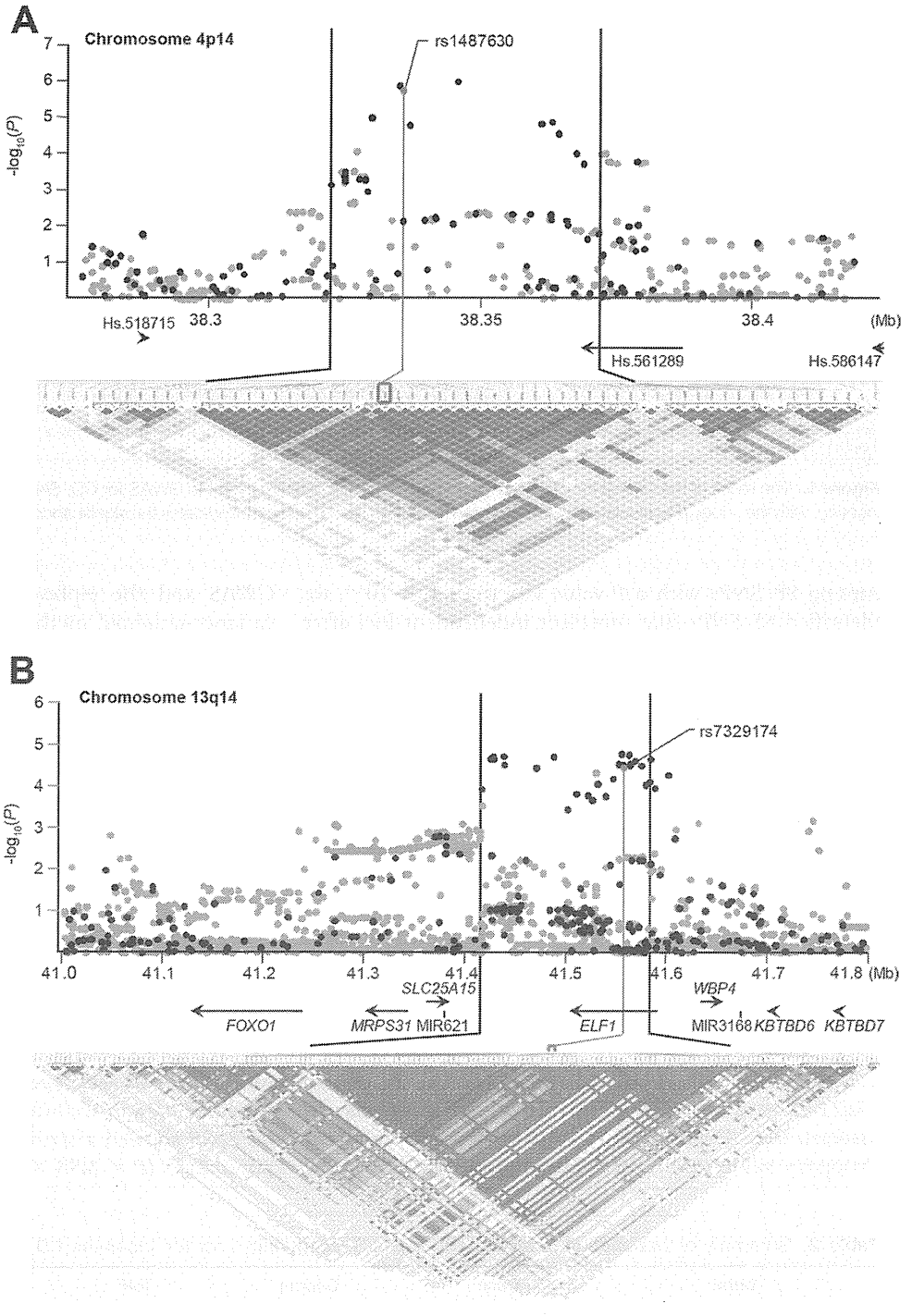

Figure 2. Case-control association results, LD map, and genomic structure of the regions on chromosomes (*A*) 4p14 and (*B*) 13q14. High-density mapping was performed in the regions (*A*) from 38.275 to 38.42 Mb on 4p14 and from (*B*) 41.35 to 41.8 Mb on 13q14. The *black dots* represent genotyped SNPs, and *gray dots* represent imputed SNPs. The *thick black line* represents the associated region defined by the LD block. The LD map based on D-prime values was drawn by using the genotype data of high-density mapping with markers of MAF greater than 0.2. The landmark SNPs on each region are indicated by a *red line*.

Fine Mapping of Two Identified Susceptibility Loci

To further characterize these susceptibility regions, we performed high-density mapping around 2 markers identified in the GWAS. First, we imputed untyped markers in the GWAS data for the region of rs1487630 (±500 kb) using the 1000 Genomes project reference haplotypes (June 2011).[29] We constructed a regional plot for the 4p14 locus (Supplementary Figure 3*B*) and narrowed down the associated region to approximately 100 kb spanning from 38.3 to 38.4 Mb on chromosome 4. To clarify the susceptibility region of 4p14, we selected and genotyped a total of 76 SNPs by a multiplex PCR-based Invader assay: 9 SNPs that showed a *P* value less than 1×10^{-4} by imputation analysis and 67 tag SNPs selected from the HapMap phase II JPT data under the criteria of r^2 greater than 0.9 and MAF greater than 0.05 (Figure 2*A*; results of an association study with genotyped data are shown in Supplementary Table 3*A*).[25] The most highly associated SNPs were located within an LD block spanning approximately

50 kb from 38.32 to 38.37 Mb on chromosome 4. This high-density mapping found 2 additional SNPs that showed similar associations with rs1487630 ($P = 1.07 \times 10^{-6}$ for rs73243354 and $P = 1.22 \times 10^{-6}$ for rs73243351; Supplementary Table 3*A*). Because these 3 SNPs were in strong LD ($r^2 > 0.85$), haplotype analysis could not detect a stronger association than the single-marker association (Supplementary Figure 4*A*).

For the second susceptibility region on chromosome 13q14, we also performed imputation around the associated marker of rs7329174 (Supplementary Figure 3*B*). Our imputation analysis found that associated variants spanned a wide region from 41.4 to 41.8 Mb on 13q14. To narrow down the candidate region around rs7329174, we genotyped a total of 190 SNPs including 33 imputed SNPs and 157 tag-SNPs (Supplementary Table 3*B*). This high-density mapping identified an additional 15 SNPs that showed the same strength of association as rs7329174, and these SNPs were located within a 174-kb LD block (Figure 1*B*). We also performed haplotype analysis with 16 highly associated SNPs, but no haplotype showed a stronger association than was observed using single markers (Supplementary Figure 4*B*).

eQTL Analysis and Pathway Analysis

To identify promising regional transcripts, we examined the effect of associated SNPs on the expression of 2 loci by using the available eQTL data.[40] On 4p14, none of these 3 SNPs affected the expression level of a likely candidate gene locus, the nearby *Toll-like receptor* (*TLR*) gene cluster (Supplementary Figure 5*A*). We also attempted to apply eQTL analysis of 16 associated SNPs to *ELF1*, *SLC25A15*, and *WBP4* around rs7329174 on 13q14. Although these SNPs did not affect the expression of *ELF1* or *WBP4*, we found that the associated SNPs upregulated the expression level of *SLC25A15* ($P = .00055$, $P_{FDR\ (False\ Discovery\ Rate)} = .0090$ between *SLC25A15* and rs7329474/rs57088152; Supplementary Figure 5*B*). These results suggest that *ELF1* or *SLC25A15* are candidate susceptibility genes for CD in this region. Further functional studies will be required to clarify the biological role to confer CD susceptibility.

We extended 2 pathway analyses by using GRAIL[34] and DAPPLE[35] to identify connections among our single-marker associations and link them with broader biological processes. As candidates for these analyses, we selected 22 SNPs: 12 variants that showed associations in this study and 10 SNPs that were replicated in our previous report.[33] To analyze the functional connections among them, we used the GRAIL method of literature-based pathway analysis to explore the connections between genes near our candidates. Six regions had significant GRAIL scores (Supplementary Table 4). This analysis indicated that there were strong connections between our 2 dominant signals at the MHC region and *TNFSF15*. The top associated region around *HLA-DQA1* was functionally related to multiple genes (Supplementary Figure 6). Subsequently, we constructed a network of proteins from these 22 loci by using DAPPLE.[35] However, neither the direct (between the associated transcripts themselves) nor the indirect (via common interactors that were not among the associated transcripts) connectivities were statistically significant ($P_{permuted}$ for direct-connectivity = .19; $P_{permuted}$ for indirect = .52; Supplementary Figure 7).

Discussion

IBD, CD, and ulcerative colitis are multifactorial diseases characterized by remitting and relapsing inflammation in the gut.[1] Although genetic differences for CD susceptibility loci are known,[18-20,33] most CD susceptibility loci were derived from cohorts of European ancestry.[7,12-14] Recently, the International IBD Genetics Consortium identified an additional 71 associations using a meta-analysis of more than 75,000 cases and controls.[44] Combined with previous reports, a total of 163 IBD loci over genome-wide significance thresholds have been identified. However, there have been few GWAS data in East-Asian populations.[6,21] Here, to explore new susceptibility loci for CD in the East-Asian population, we performed a GWAS and a replication study with a total of 1523 Japanese CD cases and 19,189 controls. As a result, we identified 2 novel loci that confer CD susceptibility in the Japanese population. By using genome-wide imputation analysis, we identified one additional candidate locus for CD susceptibility. These 3 loci did not overlap with those found in the latest report from the International IBD Genetics Consortium.[44]

Around the susceptibility region of chromosome 4p14, there are no protein-coding genes or known micro RNAs from the database miRBase (http://www.mirbase.org/). According to the UniGene database (http://www.ncbi.nlm.nih.gov/unigene), 2 expression sequence tags, Hs.518715 and Hs.561289, are mapped around this region. However, the functions of these expression sequence tags are mostly unknown. A TLR gene cluster (*TLR10*, *TLR1*, and *TLR6*) is located approximately 500 kb from the susceptibility region on the centromeric side. TLRs are primary triggers of the innate immune system by recognizing various microorganisms through conserved pathogen-associated molecular patterns.[45] Therefore, we examined the effect of the top 3 associated SNPs on the expression of the *TLR* gene cluster by using the available eQTL data.[40] However, none of these 3 SNPs affect the expression level of these genes (Supplementary Figure 5*A*).

The associated region of 13q14 encompassed the *ELF1* gene. The encoded protein of *ELF1* is implicated in the transcriptional regulation of T-cell–specific genes such as CD4 and plays an important role in the ontogeny and function of invariant natural killer T cells.[46,47] It was reported that invariant natural killer T cells provide a natural barrier against the Th17 response in a mouse model of experimental autoimmune encephalomyelitis.[48] Therefore, the *ELF1* gene is a candidate for CD susceptibility in this region. Several other genes are located around this region; MIR2276 (microRNA) and *SLC25A15*

are located on the centromeric side, and *WBP4* is located on the telomeric side. The encoded protein of *SLC25A15* transports ornithine across the inner mitochondrial membrane from the cytosol to the mitochondrial matrix. Mutations in *SLC25A15* cause hyperornithinemia-hyperammonemia-homocitrullinuria syndrome.[49] The *WBP4* gene encodes FBP21, which plays a role in the cross-intron bridging of U1 and U2 snRNPs in spliceosomal complex A.[50] By our eQTL analysis, the susceptibility alleles on 13q14 will up-regulate the expression level of *SLC25A15* (Supplementary Figure 5*B*). Further functional studies are required to clarify the biological role of this region in conferring CD susceptibility.

By performing an association study using genome-wide imputation of the GWAS subjects' data, we identified rs11894081 as a suggestive locus for conferring CD susceptibility. The nearest gene to rs11894081 was *SOX11* (sex determining region Y-box 11). Although aberrant expression of SOX11 activates histone marks in some B-cell neoplasms,[51] the relationship between *SOX11* and CD is unknown. Moreover, this association was obtained from analysis of real genotype data for cases and imputed genotype data for controls. Further studies are needed to clarify the association.

In European ancestry CD, dominant signals were observed at *NOD2* and *IL23R*, with only modest signals observed within the MHC.[13,14] In contrast, the genetic architecture of Japanese CD was dominated by 2 signals at the MHC and *TNFSF15*. For systematic comparison, we extracted the GWAS data of SNPs with nominal association ($P < .01$) in the 71 regions defined by a previous report using subjects of European descent (Supplementary Table 5).[14] Although the allele frequencies of causal variants in *NOD2* were very low in the Japanese population,[18,33] different SNPs showed nominal association in Japanese CD patients. For the *IL23R* region, there was no associated SNP in Japanese CD patients. The strong signals around the MHC class II molecules may be caused by the ethnic differences in the MHC region, as described previously.[21] The *STAT3* gene has been identified as a common susceptibility gene, but the most associated SNP in Japanese CD patients differed from that found in European populations. Our data provide details of the difference in the genetic architecture of CD between Japanese and European CD patients.

In conclusion, we identified 2 new susceptibility loci for CD at 4p14 (spanning from 38.32 to 38.37 MB) and 13q14 (spanning from 41.416 to 41.59 MB) in the Japanese population. Further functional studies of these loci will provide a better understanding of the pathogenesis of CD.

Supplementary Material

Note: To access the supplementary material accompanying this article, visit the online version of *Gastroenterology* at www.gastrojournal.org, and at http://dx.doi.org/10.1053/j.gastro.2012.12.021.

References

1. Podolsky DK. Inflammatory bowel disease. N Engl J Med 2002; 347:417–429.
2. Asakura K, Nishiwaki Y, Inoue N, et al. Prevalence of ulcerative colitis and Crohn's disease in Japan. J Gastroenterol 2009;44: 659–665.
3. Goh K, Xiao S. Inflammatory bowel disease: a survey of the epidemiology in Asia. J Dig Dis 2009;10:1–6.
4. Cho JH. The genetics and immunopathogenesis of inflammatory bowel disease. Nat Rev Immunol 2008;8:458–466.
5. Budarf ML, Labbé C, David G, et al. GWA studies: rewriting the story of IBD. Trends Genet 2009;25:137–146.
6. Yamazaki K, McGovern D, Ragoussis J, et al. Single nucleotide polymorphisms in TNFSF15 confer susceptibility to Crohn's disease. Hum Mol Genet 2005;14:3499–3506.
7. Duerr RH, Taylor KD, Brant SR, et al. A genome-wide association study identifies IL23R as an inflammatory bowel disease gene. Science 2006;314:1461–1463.
8. Rioux JD, Xavier RJ, Taylor KD, et al. Genome-wide association study identifies new susceptibility loci for Crohn disease and implicates autophagy in disease pathogenesis. Nat Genet 2007; 39:596–604.
9. Hampe J, Franke A, Rosenstiel P, et al. A genome-wide association scan of nonsynonymous SNPs identifies a susceptibility variant for Crohn disease in ATG16L1. Nat Genet 2007;39:207–211.
10. Libioulle C, Louis E, Hansoul S, et al. Novel Crohn disease locus identified by genome-wide association maps to a gene desert on 5p13.1 and modulates expression of PTGER4. PLoS Genet 2007; 3:e58.
11. Parkes M, Barrett JC, Prescott NJ, et al. Sequence variants in the autophagy gene IRGM and multiple other replicating loci contribute to Crohn's disease susceptibility. Nat Genet 2007;39:830–832.
12. The Wellcome Trust Case Control Consortium. Genome-wide association study of 14,000 cases of seven common diseases and 3,000 shared controls. Nature 2007;447:661–678.
13. Barrett JC, Hansoul S, Nicolae DL, et al. Genome-wide association defines more than 30 distinct susceptibility loci for Crohn's disease. Nat Genet 2008;40:955–962.
14. Franke A, McGovern DPB, Barrett JC, et al. Genome-wide meta-analysis increases to 71 the number of confirmed Crohn's disease susceptibility loci. Nat Genet 2010;42:1118–1125.
15. Manolio TA, Collins FS, Cox NJ, et al. Finding the missing heritability of complex diseases. Nature 2009;461:747–753.
16. Hilmi I, Tan YM, Goh KL. Crohn's disease in adults: observations in a multiracial Asian population. World J Gastroenterol 2006;12: 1435–1438.
17. Wang YF, Zhang H, Ouyang Q. Clinical manifestations of inflammatory bowel disease: East and West differences. J Dig Dis 2007;8:121–127.
18. Yamazaki K, Takazoe M, Tanaka T, et al. Absence of mutation in the NOD2/CARD15 gene among 483 Japanese patients with Crohn's disease. J Hum Genet 2002;47:469–472.
19. Yamazaki K, Onouchi Y, Takazoe M, et al. Association analysis of genetic variants in IL23R, ATG16L1 and 5p13.1 loci with Crohn's disease in Japanese patients. J Hum Genet 2007;52:575–583.
20. Yamazaki K, Takahashi A, Takazoe M, et al. Positive association of genetic variants in the upstream region of NKX2-3 with Crohn's disease in Japanese patients. Gut 2009;58:228–232.
21. Okada Y, Yamazaki K, Umeno J, et al. HLA-Cw*1202-B*5201-DRB1*1502 haplotype increases risk for ulcerative colitis but reduces risk for Crohn's disease. Gastroenterology 2011;141: 864–871.e1–5.
22. Lennard-Jones JE. Classification of inflammatory bowel disease. Scand J Gastroenterol Suppl 1989;170:2–6; discussion, 16–9.
23. Asano K, Matsushita T, Umeno J, et al. A genome-wide association study identifies three new susceptibility loci for ulcerative colitis in the Japanese population. Nat Genet 2009;41:1325–1329.

24. Nakamura Y. The BioBank Japan Project. Clin Adv Hematol Oncol 2007;5:696–697.
25. The International Hapmap Consortium. A haplotype map of the human genome. Nature 2005;437:1299–1320.
26. Yamaguchi-Kabata Y, Nakazono K, Takahashi A, et al. Japanese population structure, based on SNP genotypes from 7003 individuals compared to other ethnic groups: effects on population-based association studies. Am J Hum Genet 2008;83:445–456.
27. Okada Y, Hirota T, Kamatani Y, et al. Identification of nine novel loci associated with white blood cell subtypes in a Japanese population. PLoS Genetics 2011;7:e1002067.
28. Howie BN, Donnelly P, Marchini J. A flexible and accurate genotype imputation method for the next generation of genome-wide association studies. PLoS Genet 2009;5:e1000529.
29. The 1000 Genomes Project Consortium. A map of human genome variation from population-scale sequencing. Nature 2010;467: 1061–1073.
30. Zheng J, Li Y, Abecasis GR, et al. A comparison of approaches to account for uncertainty in analysis of imputed genotypes. Genet Epidemiol 2011;35:102–110.
31. Li Y, Willer CJ, Ding J, et al. MaCH: using sequence and genotype data to estimate haplotypes and unobserved genotypes. Genet Epidemiol 2010;34:816–834.
32. Barrett J, Fry B, Maller J. Haploview: analysis and visualization of LD and haplotype maps. Bioinformatics 2005;21:263–265.
33. Hirano A, Yamazaki K, Umeno J, et al. Association study of 71 European Crohn's disease susceptibility loci in a Japanese population. Inflamm Bowel Dis. In press.
34. Raychaudhuri S, Plenge RM, Rossin EJ, et al. Identifying relationships among genomic disease regions: predicting genes at pathogenic SNP associations and rare deletions. PLoS Genet 2009;5: e1000534.
35. Rossin EJ, Lage K, Raychaudhuri S, et al. Proteins encoded in genomic regions associated with immune-mediated disease physically interact and suggest underlying biology. PLoS Genet 2011; 7:e1001273.
36. Bakker PIW de, Ferreira MAR, Jia X, et al. Practical aspects of imputation-driven meta-analysis of genome-wide association studies. Hum Mol Genet 2008;17:R122–R1228.
37. Price AL, Patterson NJ, Plenge RM, et al. Principal components analysis corrects for stratification in genome-wide association studies. Nat Genet 2006;38:904–909.
38. Gabriel SB, Schaffner SF, Nguyen H, et al. The structure of haplotype blocks in the human genome. Science 2002;296:2225–2229.
39. Purcell S, Neale B, Todd-Brown K, et al. PLINK: a tool set for whole-genome association and population-based linkage analyses. Am J Hum Genet 2007;81:559–575.
40. Stranger BE, Forrest MS, Dunning M, et al. Relative impact of nucleotide and copy number variation on gene expression phenotypes. Science 2007;315:848–853.
41. Danecek P, Auton A, Abecasis G, et al. The variant call format and VCFtools. Bioinformatics 2011;27:2156–2158.
42. Yang J, Yang W, Hirankarn N, et al. ELF1 is associated with systemic lupus erythematosus in Asian populations. Hum Mol Genet 2011;20:601–607.
43. Okada Y, Shimane K, Kochi Y, et al. A genome-wide association study identified AFF1 as a susceptibility locus for systemic lupus eyrthematosus in Japanese. PLoS Genet 2012;8:e1002455.
44. Jostins L, Ripke S, Weersma RK. Host-microbe interactions have shaped the genetic architecture of inflammatory bowel disease. Nature 2012;490:119–124.
45. Kawai T, Akira S. The role of pattern-recognition receptors in innate immunity: update on Toll-like receptors. Nat Immunol 2010;11:373–384.
46. Sarafova S, Siu G. A potential role for Elf-1 in CD4 promoter function. J Biol Chem 1999;274:16126–16134.
47. Choi H-J, Geng Y, Cho H, et al. Differential requirements for the Ets transcription factor Elf-1 in the development of NKT cells and NK cells. Blood 2011;117:1880–1887.
48. Mars LT, Araujo L, Kerschen P, et al. Invariant NKT cells inhibit development of the Th17 lineage. Proc Natl Acad Sci U S A 2009;106:6238–6243.
49. Camacho JA, Obie C, Biery B, et al. Hyperornithinaemia-hyperammonaemia-homocitrullinuria syndrome is caused by mutations in a gene encoding a mitochondrial ornithine transporter. Nat Genet 1999;22:151–158.
50. Bedford MT, Reed R, Leder P. WW domain-mediated interactions reveal a spliceosome-associated protein that binds a third class of proline-rich motif: the proline glycine and methionine-rich motif. Proc Natl Acad Sci U S A 1998;95:10602–10607.
51. Vegliante MC, Royo C, Palomero J, et al. Epigenetic activation of SOX11 in lymphoid neoplasms by histone modifications. PLoS One 2011;6:e21382.

Received April 16, 2012. Accepted December 17, 2012.

Reprint requests

Address requests for reprints to: Michiaki Kubo, MD, PhD, Laboratory for Genotyping Development, Center for Genomic Medicine, Riken Yokohama Institute, 1-7-22 Suehiro-Cho, Tsurumi-Ku, Yokohama, Kanagawa 230-0045, Japan. e-mail: mkubo@src.riken.jp; fax: (81) 45-503-9606.

Acknowledgments

The authors thank the members of the BioBank Japan project and the Rotary Club of Osaka-Midosuji District 2660 Rotary International in Japan; all patients with Crohn's disease and their families for their contribution to this project; and Ai Maejima, Mayumi Nakayama, Takako Tokugawa, Yuko Sumikawa, Kyota Ashikawa, Tomomi Aoi, and the other members of the Laboratory for Genotyping Development for their technical assistance.

Conflicts of interest

The authors disclose no conflicts.

Funding

Supported by a grant from the BioBank Japan Project and in part by a Grant-in-Aid for Young Scientists (A) (22689025) from the Ministry of Education, Culture, Sports, Science and Technology.

OPEN ACCESS

ORIGINAL ARTICLE

Bone marrow-mesenchymal stem cells are a major source of interleukin-7 and sustain colitis by forming the niche for colitogenic CD4 memory T cells

Yasuhiro Nemoto,[1] Takanori Kanai,[2] Masahiro Takahara,[1] Shigeru Oshima,[1] Tetsuya Nakamura,[1] Ryuichi Okamoto,[1] Kiichiro Tsuchiya,[1] Mamoru Watanabe[1]

▶ Additional supplementary data are published online only. To view these files please visit the journal online (http://dx.doi.org/10.1136/gutjnl-2012-302029).

[1]Department of Gastroenterology and Hepatology, Graduate School, Tokyo Medical and Dental University, Tokyo, Japan
[2]Division of Gastroenterology and Hepatology, Department of Internal Medicine, Keio University School of Medicine, Tokyo, Japan

Correspondence to
Professor Mamoru Watanabe, Department of Gastroenterology and Hepatology, Tokyo Medical and Dental University, 1-5-45 Yushima, Bunkyo-ku, Tokyo 113-8510, Japan; mamoru.gast@tmd.ac.jp

Received 21 September 2012
Accepted 7 October 2012
Published Online First 9 November 2012

ABSTRACT

Objective Interleukin (IL)-7 is mainly produced in bone marrow (BM) that forms the niche for B cells. We previously demonstrated that BM also retains pathogenic memory CD4 T cells in murine models of inflammatory bowel disease (IBD). However, it remains unknown whether BM-derived IL-7 is sufficient for the development of IBD and which cells form the niche for colitogenic memory CD4 T cells in BM.

Design To address these questions, we developed mice in which IL-7 expression was specific for BM, and identified colitis-associated IL-7-expressing mesenchymal stem cells (MSC) in the BM.

Results IL-7$^{-/-}$×RAG-1$^{-/-}$ mice injected with BM cells from IL-7$^{+/+}$×RAG-1$^{-/-}$ mice, but not from IL-7$^{-/-}$×RAG-1$^{-/-}$ mice, expressed IL-7 in BM, but not in their colon, and developed colitis when injected with CD4^{+}CD45RB^{high} T cells. Cultured BM MSC stably expressed a higher level of IL-7 than that of primary BM cells. IL-7-sufficient, but not IL-7-deficient, BM MSC supported upregulation of Bcl-2 in, and homeostatic proliferation of, colitogenic memory CD4 T cells in vitro. Notably, IL-7$^{-/-}$×RAG-1$^{-/-}$ mice transplanted with IL-7-sufficient, but not IL-7-deficient, BM MSC expressed IL-7 in BM, but not in their colon, and developed colitis when transplanted with CD4^{+}CD45RB^{high} T cells.

Conclusions We demonstrate for the first time that BM MSC are a major source of IL-7 and play a pathological role in IBD by forming the niche for colitogenic CD4 memory T cells in BM.

Significance of this study

What is already known on this subject?

- IL-7 is mainly produced in BM.
- BM stromal cells forms the niche for B cells.
- We have previously reported that colitogenic memory CD4 T cells are retained in BM of IBD model mice in a IL-7-dependent manner.
- MSC have the ability to downmodulate inflammation and improve tissue repair, so their use to treat inflammatory diseases is being explored.

What are the new findings?

- IL-7$^{-/-}$×RAG-1$^{-/-}$ mice injected with BM cells from IL-7$^{+/+}$×RAG-1$^{-/-}$ mice, but not from IL-7$^{-/-}$×RAG-1$^{-/-}$ mice, expressed IL-7 in BM, but not in the colon, and developed colitis when injected with CD4^{+}CD45RB^{high} T cells.
- BM MSC produced larger amount of IL-7 than that of primary BM cells.
- IL-7-sufficient, but not IL-7-deficient, BM MSC supported upregulation of Bcl-2 in, and homeostatic proliferation of, colitogenic memory CD4 T cells in vitro.
- IL-7$^{-/-}$×RAG-1$^{-/-}$ mice transplanted with IL-7-sufficient, but not IL-7-deficient, BM MSC expressed IL-7 in BM, but not in the colon, and developed colitis when transplanted with CD4^{+}CD45RB^{high} T cells.

How might it impact on clinical practice in the foreseeable future?

- The present study may be a new example for changing concepts of IBD from intestinal to systemic disease, and a therapeutic approach targeting BM MSC-derived IL-7 may be feasible in the treatment of chronic immune diseases.

Open Access
Scan to access more free content

Linked

▶ http://dx.doi.org/10.1136/gutjnl-2012-303903

To cite: Nemoto Y, Kanai T, Takahara M, *et al*. *Gut* 2012;**62**:1142–1152.

INTRODUCTION

Inflammatory bowel disease (IBD) is characterised by chronic inflammation of the gastrointestinal tract. Accumulating evidence suggests that IBD is caused by an inappropriate response of the innate and acquired immune systems to commensal microbiota.[1] Even if IBD enters remission as a result of treatment, it often relapses, leading to its lifelong duration. Therefore, we hypothesised that even in remission, colitogenic memory T cells survive for a long period as 'pathogenic memory stem cells'[2 3] in IBD patients.

Interleukin (IL)-7 is an important cytokine involved in supporting the survival of naive and memory, but not effector, CD4 T cells.[4–6] IL-7 is secreted by stromal cells in the bone marrow (BM) and thymus, and by epithelial cells.[7] In a series of studies, we have consistently focused on IL-7 as an essential factor for the persistence of chronic T-cell-mediated colitis. We have shown that: (1) IL-7 is constitutively produced by intestinal goblet cells;[8] (2) IL-7 transgenic mice, in which strong promoters drive systemic overexpression, develop colitis that mimics the histopathological characteristics of human IBD;[9] (3) colitogenic CD4 effector memory T (T_{EM}) cells, which express high levels of IL-7Rα, reside in the inflamed lamina propria (LP)

of RAG-2$^{-/-}$ mice injected with CD4$^+$CD45RB^{high} T cells;[10] and (4) IL-7$^{-/-}$×RAG-1$^{-/-}$ mice injected with CD4$^+$CD45RB^{high} T cells or colitogenic LP CD4$^+$ T_{EM} cells do not develop colitis.[11]

However, we have found that the IL-7 level of colitic intestine is less than that of normal intestine as a result of the disappearance of goblet cells.[12] Therefore, we hypothesise that colitogenic memory CD4 T cells are maintained outside the intestine as memory stem cells. Because the spleen and lymph nodes are dispensable for the development of chronic colitis,[13] we found that BM is the main source of IL-7.[14 15] We previously demonstrated that, in addition to a major subpopulation of T_{EM} cells, a substantial proportion of colitogenic CD4 central memory cells preferentially reside in the BM of colitic mice.[16 17] Importantly, these resident BM CD4 memory T cells are closely associated with IL-7-producing stromal cells and retain a significant potential to induce colitis after adoptive retransfer into new SCID/RAG-2$^{-/-}$ mice. BM CD4 memory T cells cannot induce colitis when they are transferred into IL-7$^{-/-}$×RAG-1$^{-/-}$ mice, suggesting that IL-7 plays an essential role in the maintenance of CD4 memory T cells in BM.[16] Using intrarectal administration of CD4 T cells, we also demonstrated that colitogenic memory CD4 T cells constantly recirculate from the LP to BM.[18]

However, two important questions remain: whether BM-derived IL-7 is sufficient for the maintenance of colitogenic CD4 memory T cells in the absence of IL-7 produced at other sites, and which cells in BM mainly produce IL-7 and form the niche for colitogenic memory CD4 T cells. To address these questions, we established mice in which IL-7 expression is specific to BM, and attempted to identify the IL-7-expressing cells in BM. Although it is generally accepted that mesenchymal stem cells (MSC) have the ability to downregulate inflammation, and their use to treat inflammatory diseases is being explored, we propose a new hypothesis in which BM MSC,[19–21] a candidate for the IL-7-producing stromal cells or their progenitors in BM, play a pathological role in the maintenance of colitogenic CD4 memory T cells.

MATERIALS AND METHODS

Animals

C57BL/6 mice were purchased from Japan CLEA (Tokyo, Japan). RAG-2-deficient mice (RAG-2$^{-/-}$) were obtained from Taconic Laboratory (Hudson, New York, USA) and Central Laboratories for Experimental Animals (Kawasaki, Japan). RAG-1$^{+/-}$ and IL-7$^{+/-}$ mice on the C57BL/6 background were kindly provided by Dr Rose Zamoyska (National Institute for Medical Research, London, UK). These mice were intercrossed to generate RAG-1$^{-/-}$ and IL-7$^{-/-}$×RAG-1$^{-/-}$ littermate mice. All mice are originally derived from C57BL/6 mice. Mice were maintained under specific pathogen-free conditions in the Animal Care Facility of Tokyo Medical and Dental University. Donors and recipients were used at 6–12 weeks of age. All experiments were approved by the regional animal study committees and performed according to institutional guidelines and Home Office regulations.

See 'more information' in supplementary materials and methods (available online only) for details.

RESULTS

IL-7$^{-/-}$× RAG-1$^{-/-}$ mice transplanted with BM cells from RAG-1$^{-/-}$ mice develop colitis after adoptive transfer of CD4$^+$CD45RB^{high} T cells

We first assessed whether BM-derived IL-7 is sufficient for the development of colitis in the absence of IL-7 produced at other sites. To this end, we used a model of chronic colitis induced by the adoptive transfer of CD4$^+$CD45RB^{high} T cells into RAG-1$^{-/-}$ mice in combination with bone marrow transplantation (BMT) of donor BM cells from RAG-1$^{-/-}$ or IL-7$^{-/-}$×RAG-1$^{-/-}$ littermate mice. First, RAG-1$^{-/-}$ and IL-7$^{-/-}$×RAG-1$^{-/-}$ mice were treated with intraperitoneal busulfan and underwent total body irradiation to ablate their BM. The next day, mice were reconstituted with donor BM cells from RAG-1$^{-/-}$ or IL-7$^{-/-}$×RAG-1$^{-/-}$ mice. Mice were divided into four groups as follows (figure 1A): IL-7$^{-/-}$×RAG-1$^{-/-}$ mice transplanted with RAG-1$^{-/-}$ BM cells (IL-7$^{+/+}$ → IL-7$^{-/-}$); IL-7$^{-/-}$×RAG-1$^{-/-}$ mice transplanted with IL-7$^{-/-}$×RAG-1$^{-/-}$ BM cells (IL-7$^{-/-}$ → IL-7$^{-/-}$); RAG-1$^{-/-}$ mice transplanted with RAG-1$^{-/-}$ BM cells (IL-7$^{+/+}$ → IL-7$^{+/+}$) and RAG-1$^{-/-}$ mice transplanted with IL-7$^{-/-}$×RAG-1$^{-/-}$ BM cells (IL-7$^{-/-}$ → IL-7$^{+/+}$). Four weeks after recovery from BMT, all groups of mice were injected intraperitoneally with CD4$^+$CD45RB^{high} T cells (figure 1A). As expected, IL-7$^{+/+}$ → IL-7$^{+/+}$ mice developed severe colitis. Interestingly, IL-7$^{-/-}$ → IL-7$^{+/+}$ mice also developed colitis at a level similar to that of IL-7$^{+/+}$ → IL-7$^{+/+}$ mice (figure 1B–E), indicating that non-hematopoietic cells, including IL-7-producing BM stromal cells and/or BM stem cells that differentiated into IL-7-producing stromal cells, could not be completely ablated by the current busulfan/irradiation protocol. In contrast, IL-7$^{-/-}$ → IL-7$^{-/-}$ mice did not develop colitis because of the lack of IL-7 (figure 1B–E). However, to our surprise, the clinical findings revealed that IL-7$^{+/+}$ → IL-7$^{-/-}$ mice injected with CD4$^+$CD45RB^{high} T cells developed a wasting disease and severe colitis to a similar extent to that of control IL-7$^{+/+}$ → IL-7$^{+/+}$ mice (figure 1B–E), indicating that the BMT protocol led to successful transplantation of IL-7-producing BM cells in IL-7$^{+/+}$ → IL-7$^{-/-}$ mice.

A quantitative evaluation of T-cell expansion was performed by counting LP, spleen and BM CD4 T cells. While only a few CD4 T cells were recovered from all sites examined in IL-7$^{-/-}$ → IL-7$^{-/-}$ mice, approximately 100-fold higher numbers of LP, spleen and BM CD4 T cells were recovered from IL-7$^{+/+}$ → IL-7$^{-/-}$, IL-7$^{+/+}$ → IL-7$^{+/+}$ and IL-7$^{-/-}$ → IL-7$^{+/+}$ mice (figure 1F). In addition, on in-vitro stimulation, LP CD4 T cells from IL-7$^{+/+}$ → IL-7$^{-/-}$, IL-7$^{+/+}$ → IL-7$^{+/+}$ and IL-7$^{-/-}$ → IL-7$^{+/+}$ mice produced equal and significantly higher amounts of interferon (IFN)-γ, tumour necrosis factor (TNF)α and IL-17 than those from IL-7$^{-/-}$ → IL-7$^{-/-}$ mice (figure 1G). Flow cytometric analysis revealed that the CD4 T cells isolated from the LP, mesenteric lymph nodes, spleen and BM of all recipients at 8 weeks after transfer of CD4$^+$CD45RB^{high} T cells had a characteristic CD69$^+$IL-7Rα^{high} phenotype (see supplementary figure S1, available online only), indicating that the transferred CD4$^+$CD45RB^{high} T cells differentiated into activated T_{EM} cells irrespective of the presence of IL-7. These results suggest that BM-derived IL-7 promotes the development and persistence of colitis primarily by supporting the expansion of colitogenic CD4 T_{EM} cells in the colon.

We performed highly sensitive reverse transcription PCR for the detection of IL-7 messenger RNA using samples obtained from the BM and colon. As shown in figure 1H, IL-7 mRNA was detected in the BM of IL-7$^{+/+}$ → IL-7$^{-/-}$, IL-7$^{+/+}$ → IL-7$^{+/+}$ and IL-7$^{-/-}$ → IL-7$^{+/+}$ mice with colitis, but not in that of IL-7$^{-/-}$ → IL-7$^{-/-}$ mice without colitis. Of note, IL-7 mRNA was detected in the LP of IL-7$^{+/+}$ → IL-7$^{+/+}$ and IL-7$^{-/-}$ → IL-7$^{+/+}$ mice, but not in IL-7$^{+/+}$ → IL-7$^{-/-}$ or IL-7$^{-/-}$ → IL-7$^{-/-}$ mice regardless of the development of colitis, indicating that after BMT, IL-7$^{+/+}$ BM cells led to the establishment of IL-7-producing stromal cells in BM. Consistent with this result, immunohistochemistry revealed that IL-7 was in the BM of IL-7$^{+/+}$ → IL-7$^{-/-}$, IL-7$^{+/+}$ → IL-7$^{+/+}$ and IL-7$^{-/-}$ → IL-7$^{+/+}$ mice with colitis, but not in IL-7$^{-/-}$ → IL-7$^{-/-}$ mice without colitis (figure 1I). However, IL-7 protein

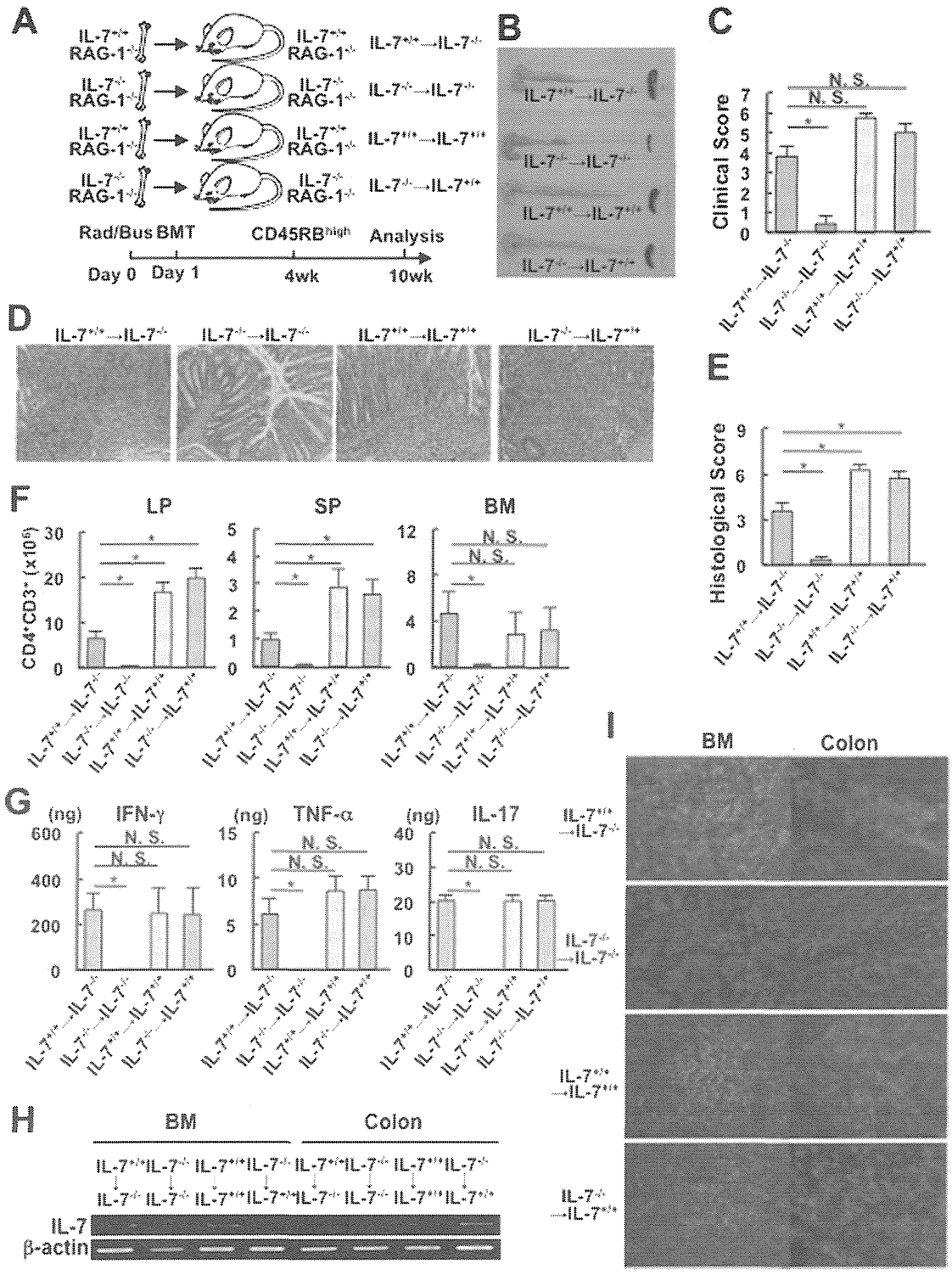

Figure 1 $CD4^+CD45RB^{high}$ T-cell-injected IL-$7^{-/-}$×RAG-$1^{-/-}$ recipients pretransplanted with bone marrow (BM) cells from IL-$7^{+/+}$×RAG-$1^{-/-}$ mice develop colitis. (A) Experimental design. Mice were divided into four groups (n=8). Each group was injected intraperitoneally with $CD4^+CD45RB^{high}$ T cells at 4 weeks after bone marrow transplantation. (B) Gross appearance of the colon, mesenteric lymph nodes and spleen (SP) from mice of each group at 10 weeks after cell administration. (C) Clinical scores determined at 10 weeks after administration as described in Materials and methods section. Data are shown as the mean±SEM for eight mice in each group, *p<0.01. (D) Histopathology of the distal colon of the indicated mice. Original magnification, ×200. (E) Histological scores. Data are shown as the mean±SEM for eight mice in each group, *p<0.05. (F) Absolute number of lamina propria (LP) $CD3^+CD4^+$ T cells from the colon. Data are shown as the mean±SEM. N.S., not significant, *p<0.01. (G) Cytokine production by LP CD4 T cells. LP CD4 T cells were isolated and stimulated in vitro. IFN-γ, TNFα and IL-17 concentrations in culture supernatants were measured by ELISA. Data are shown as the mean±SEM for eight mice in each group, *p<0.05. (H) Expression of IL-7 mRNA in colonic BM and the colon from the indicated mice as detected by reverse transcription PCR. (I) Frozen sections of BM and the colon from each mouse were stained with a polyclonal anti-IL-7 antibody. Original magnification ×400.